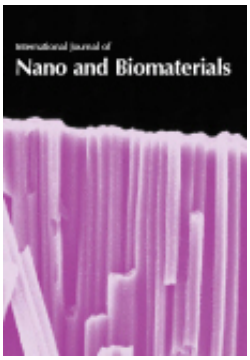

International Journal of Nano and Biomaterials

ISSN online: 1752-8941 - ISSN print: 1752-8933
https://www.inderscience.com/ijnbm

Synthesis and characterisation of iron oxide nanoparticles with thymoquinone

Sheshadri S. Temkar, M. Tarun, Seema Tharannum, M.S. Dinesh

DOI: 10.1504/IJNBM.2023.10058901

Article History:

Received:	29 March 2023
Last revised:	30 May 2023
Accepted:	20 June 2023
Published online:	02 April 2024

Synthesis and characterisation of iron oxide nanoparticles with thymoquinone

Sheshadri S. Temkar* and M. Tarun

Department of Biotechnology,
PES University,
Bangalore, Karnataka, 560085, India
Email: Temkarsheshadri@gmail.com
Email: tarunhsr955@hotmail.com
*Corresponding author

Seema Tharannum

Department of Biotechnology,
Dayanand Sagar University,
Bangalore Karnataka, 560079, India
Email: seematharannum@dsu.edu.in

M.S. Dinesh

Department of Biotechnology,
PES University,
Bangalore, Karnataka, 560085, India
Email: dineshms@pes.edu

Abstract: *Nigella sativa* is a medicinal plant used for its antimicrobial properties. Thymoquinone (TQ), being the lead component of these plant seeds, exerts antibacterial, antifungal and antioxidant activity. It has also shown promising activity against cancer and inflammation through different modes of action. In recent developments for new applications in the field of medicine, nanotechnology has excelled as a very prominent and important field. Nanoparticles are generally in the dimension range of 1–100 nm. Iron oxide nanoparticles show enhanced antibacterial activity against gram-negative bacteria. The current research focuses on comparing the yield and stability of thymoquinone-synthesised iron oxide nanoparticles using different organic solvents, the benefits expressed by thymoquinone as a herbal drug, a novel approach to the green synthesis of iron oxide nanoparticles with thymoquinone, and testing for their stability, size and functional groups.

Keywords: iron oxide nanoparticles; *Nigella sativa*; thymoquinone (TQ); preparatory high-pressure liquid chromatography; FTIR analysis; zeta potential; DLS; dynamic light scattering.

Reference to this paper should be made as follows: Temkar, S.S., Tarun, M., Tharannum, S. and Dinesh, M.S. (2024) 'Synthesis and characterisation of iron oxide nanoparticles with thymoquinone', *Int. J. Nano and Biomaterials*, Vol. 10, No. 3, pp.141–159.

Biographical notes: Sheshadri S. Temkar completed his undergraduate study in the field of Biotechnology at PES University, Bangalore, India. He has successfully interned at some of the best research institutes in India like CSIR – Institute of Genomics and Integrative Biology where he worked on SARS CoV-2 and its proof-reading mechanism and at Sri Ramachandra Medical College where he was trained in the fields of plant tissue culture. He has developed a keen interest in the field of cellular and molecular biology and has successfully published a first author paper on Breast cancer.

M. Tarun is currently pursuing Masters in Medical Biotechnology, University of Technology Sydney. He has completed his Bachelor of Technology in Biotechnology, PES University Bangalore, India 2023 and specialised in Medical & Environmental Biotechnology domain and has theoretical and practical knowledge in subjects that include nanobiotechnology, microbiology, biochemistry, toxicology, environmental biotechnology. Apart from academics he has completed internships in 'Ameliorate Biotech Pvt. Ltd.' for the project 'Optimization of Biosensor Formulation for glucose estimation of Saliva,' and has also interned in 'Dr. Reddy's Laboratories'in Quality Control department.

Seema Tharannum is currently serving as Professor of Biological sciences at School of Engineering, Dayananda Sagar University. She obtained her Master of Science in Biotechnology from Mysore University, Master of Philosophy in Biotechnology from Bharathidasan University, and a PhD in Biotechnology from Kuvempu University. She has a total experience of 28 years in teaching and research. She had two funded projects, Principal Investigator for a UGC minor research project for "Microbial mediated remediation of chromium in electroplating industry" for 1.5 Lakhs (2011–2013) and Co investigator for a CDAC sponsored project 'Detection of Pebrine spores' (2014)

M.S. Dinesh is presently working as an Associate Professor at the Department of Biotechnology, PES University, Bangalore, India. He carried out research on Nano Biofertilizers and Biopesticides for sustainable environment at Indian Institute of Horticultural Research. His Post-Doctoral work involved nano functionalised antimicrobial peptides as fungicides at Indian Institute of Science, Bangalore, India.

1 Introduction

Currently, we are in the era of "End to Modern Medicine if bacteria can resist" (Yoshikawa, 2002) Antibiotic-resistant bacteria are bacteria that are not controlled or killed by antibiotics. They are able to survive and even multiply in the presence of an antibiotic. Most bacteria that cause infections are capable of developing resistance to at least some drugs. Antibiotics that were once often used to treat microorganisms have become ineffective against some of them. For instance, *Neisseria gonorrhoeae* (the cause of gonorrhea) and *Staphylococcus aureus* (often known as 'golden staph' or MRSA) are now virtually always resistant to *benzylpenicillin*. In the past, penicillin was typically used to treat these illnesses (Department of Health and Human Services, no date; [No title]).

An experiment was conducted by Stuart B Levy (2005) where three geographically separated patients treated with the antibiotic Vancomycin were subjected to the harmful effects of the bacteria *Staphylococcus aureus*, to conclude the antibiotic was ineffective

against the bacteria ('Antibiotic resistance–the problem intensifies', 2005; Howden et al., 2010). Gram-negative bacterial species have a cell wall which consists of lipopolysaccharides. They are a large unique class of macromolecules found in the outer layer of the cell wall and are involved in the interaction of the cell with the external environment.

Due to the permeability barrier exhibited by its external layer, gram-negative species such as *P. aeruginosa* and *E. coli* are resistant to many drugs (Zgurskaya et al., 2015). Gram-negative bacteria have become extremely adept at picking up antibiotic-resistant determinants from one another as well as from their environment, leading to widespread antibiotic resistance. In the intensive care unit, certain Gram-negative microbes, such as *Pseudomonas aeruginosa*, *Acinetobacter spp.*, *Stenotrophomonas maltophilia*, and the *Enterobacteriaceae*, are particularly problematic (Waterer and Wunderink, 2001). The combination of a rising risk population and Gram-negative bacteria's intrinsic virulence and adaptability ensures that critical care physicians face a constant and escalating threat from these diseases. Organisms have developed a wide range of mechanisms to prevent and resist the action of many antimicrobials and antibacterial drugs used in clinical medicine. Some of the mechanisms of resistance include efflux pumps, alteration of the drug binding site and membrane permeability, degradation enzymes, and the conformational change of the drug culminating in its inactivation (Oliveira and Reygaert, 2019) . Herbal medicines are in great demand against diseases and disorders because of their efficacy, safety and low side effects. They also offer therapeutics for age-related disorders like memory loss, immune disorders etc. (Website, no date).

Nigella sativa is a medical plant used for its antibacterial/antimicrobial property. One of the main components of this plant is Thymoquinone (TQ), which is the reason for its antimicrobial activity against gram-positive and gram-negative bacteria (Ahmad et al., 2013; Ali and Blunden, 2003). Nanomedicine is the application of nanotechnology to the field of medicine. The average size of iron oxide nanoparticles found by dynamic light scattering (DLS) particle size analyser, ranges approximately between 10 nm to 120 nm with a mean particle size of 66 nm. Nanoparticles exert a few important attributes like nanoscale size, high surface-to-mass ratio, and high reactivity. Due to these characteristics, they are suitable candidates for various applications, which include catalysis, medical imaging, medical applications, energy-based research, and environmental applications ('Nanoparticles: Properties, applications and toxicities', 2019). High amounts of bacterial toxicity mechanisms have been observed in metal-based nanoparticles which collectively makes it difficult for the development of resistance and results in broadening the array of antibacterial activity (Dinali et al., 2017; Tran et al., 2010). The development of nanoparticles has been at the forefront in the last decade using a variety of processes like co-precipitation, thermal decomposition, hydrothermal synthesis, microemulsion, sonochemical synthesis, and sonochemical synthetic routes. Iron oxide nanoparticles show enhanced antibacterial activity against gram-negative bacteria, in our project we mainly focus on this property of nanoparticles (Ali et al., 2016).

1.1 Nigella sativa

Herbal medicine or phytotherapy is a domain of medical science where there is the use of herbal remedies to treat the sick. It covers areas from medicinal plants with powerful actions, such as Digitalis and Belladonna, to those with very gentle actions, such as

chamomile, mint, and many others. Research and analysis on a group of plants have been done for their medicinal properties, out of which *Nigella sativa* has emerged to be a herb with rich historical and traditional backgrounds (Ali and Blunden, 2003).

Nigella sativa (*N. sativa*) which is cultivated in different parts of the world has been used as a remedy to treat several diseases. The seeds of this plant consist of proteins, carbohydrates, crude fibres, alkaloids, saponins, ash, and fixed oils (Shokri, 2016).

The pH of *N. sativa* seeds is around 5.6–5.7 or sometimes slightly lower than that which indicates its slightly acidic (Łopusiewicz et al., 2022). Reports have been generated on several activities of this plant, which include antioxidant and anti-inflammatory agents and furthermore used as an antihypertensive and anti-microbial agent. Studies on *N. sativa* has led to the discovery of a wide array of its pharmacological activity by multiple researchers (Ahmad et al., 2013). The seeds consist of saponins, alkaloids and proteins, the antimicrobial activity is due to the presence of a component called Thymoquinone. The oil assists in decreasing blood pressure and increasing respiration. Rats treated with the seed extract for a period of 12 weeks showed signs of reduction in triglycerides, cholesterol and glucose. Use of either the seed extract or its oil has no impact on liver or kidney functions in the human body (Ali and Blunden, 2003).

1.2 Morphology of the plant

N. sativa is an annual flowering plant which grows up to a height of 20–90 cm with growth, proliferation, flowering, seeding and death in one single season of spring and early summer. They have finely separated leaves, with diverse colours of flowers in white, yellow, pink, pale blue or pale purple, with 7–10 petals. The fruit is a large and inflated capsule composed of 4–8 united follicles each containing large amounts of seeds (Ahmad et al., 2013).

1.3 Physical property of the seed

The seeds are small-scaled, bi-lobed, black externally and white internally, they have a slight aroma to them and a bitter taste. On a microscopic level, the sagittal plane of the seed depicts a mono-layered epidermis containing an elliptically thick-walled papillose cuticle composed of dark brown matter. This is followed by two- four layers of parenchymatous cells and finally, a sepia-pigmented layer containing thick-walled rectangular lengthened cells. Endosperm comprises narrow rectangular cells mostly composed of oil spheres (Ahmad et al., 2013).

Thymoquinone Proteins and amino acids, carbohydrates, alkaloids, organic acids, saponins, crude fibres, vitamins and minerals are the varieties of chemical compounds found in *N. sativa* seeds. Thymoquinone with a chemical name of 2-isopropyl-5-methylbenzo-1, 4-quinone has been identified as a phytochemical complex found excessively in *N. sativa* seeds and oil. It was first identified and extracted by El-Dakhakhny by performing thinlayer chromatography on a silica-coated TLC plate (‘Thymoquinone and its therapeutic potentials’, 2015). Thymoquinone has great potential as an anti-oxidant, anti-bacterial, anti-fungal and anti-inflammatory compound. The active compounds found in these seeds are thymoquinone, thymohydroquinone, dithymoquinone (nigellone), thymol, carvacrol, nigellicine, nigellidine and α-hedrin. Thymoquinone exists in a tautomeric form and there is a presence of a keto group in high concentration due to which there are effects of pharmacological activity in them. It is a

natural compound and has received high amounts of interest and focus due to its therapeutic properties ('Thymoquinone: Potential cure for inflammatory disorders and cancer', 2012). However, thymoquinone as a separate biomolecule is unstable due to its poor water solubility, leading to low absorptivity and bioavailability. Therefore, it has to be dissolved in a suitable solvent like DMSO without altering its capability (Tubesha et al., 2013).

1.4 Antibacterial activity

Many papers support the fact that *N. sativa* prevents the formation of biofilms. Thymoquinone, a highly useful compound in *N. sativa* shows broad-spectrum activity against several strains of bacteria. For species like *Staphylococcus aureus* and *Staphylococcus epidermidis* biofilm inhibition has been observed at 22 micrograms per milli-litre and 60 micrograms per milli-litre (Balyan et al., 2021).

1.5 Antifungal activity

Aspergillus fumigatus and Aspergillus flavus fungal growth inhibition has been analysed and proven when there is a presence of plant extract. *Trichophyton mentagrophytes*, *Microsporum gypseum*, and *Microsporum canis* are pathogenic dermatophyte strains that *N. sativa* extract has shown antifungal action against. In an in-vivo investigation, mice were infected with *Candida albicans* a pathogenic yeast present in the human gut microflora which was then treated with an aqueous extract of black seeds. Author The extract showed inhibiting activity towards fungal growth activity in them (Forouzanfar et al., 2014) On performing a different treatment experiment for Candida-related infection with *Nigella sativa* extracts, the antifungal effect was assessed by measuring the zone of inhibition. These results indicated that the methanolic extracts of *Nigella sativa* had a strong antifungal effect followed by the chloroform extract and the aqueous extract showed no zone of inhibition (Bita et al., 2012).

1.6 Antioxidant

Activity Use of natural antioxidant compounds has gained popularity for their ability to quench their free radical to protect the human body against oxidative stress. Thymoquinone has shown promising activity against reactive oxygen species (ROS) like superoxide anions and hydroxyl radicals and thus reducing their effects on the human body. The presence of quinone structure is the main reason for the anti-oxidative property shown by this compound. Thymoquinone also showed protection against several organs from oxidative damage by inducing several free radical-generating agents ('Thymoquinone and its therapeutic potentials', 2015).

1.7 Iron oxide nanoparticles

1.7.1 Size range of nanoparticles

On average iron oxide nanoparticles have a size range of approximately 10–120 nm with a mean particle size of 66 nm (View of Synthesis and Characterization of Magnetic Iron Oxide Nanoparticles by Co-Precipitation Method at Different Conditions, no date a)

1.7.2 Application of nanoparticles

Nanomedicine refers to the use of nanotechnology in the field of medical science. Some of the special characteristics of nanomaterials include their nanoscale size, high surface-to-mass ratio, and high reactivity. Nanoparticles find their applications in the fields of life sciences like biomedicine, agriculture, and the environment, iron oxide has immense potential (Sun et al., 2021; Anjum et al., 2021).

1.7.3 Iron oxide nanoparticles

Iron oxide is formed by chemically combining iron and oxygen. In nature, iron (III) oxide is found in the form of rust. Generally, iron oxides are prevalent, widely used as they are inexpensive, and play an imperative Title role in many biological and geological processes. High amounts of bacterial toxicity mechanisms have been observed in metal-based nanoparticles which collectively make it difficult for the development of resistance and result in broadening the array of antibacterial activity. Due to their low toxicity, superparamagnetic properties, such as surface area and volume ratio, and simple separation methodology, magnetic iron oxide (Fe3O4 and Fe2O3) NPs have attracted much attention and found their use in biomedical applications (Ali et al., 2016)

1.7.4 Anti-cancer property

Nanoparticles' size, shape, and surface characteristics are crucial for achieving targeted anticancer activity with minimum complexity. Due to a retention effect and increased vascular permeability, nanoparticles can penetrate tumour cells with ease. Nanoparticles are frequently spherical in shape because of how easily they can be manufactured. By emitting harmless wavelength radiation that is easily absorbed by dangerous stimuli that lead to the creation of reactive oxygen species, iron oxide nanoparticles both directly and indirectly exhibit anticancer activity (Sun et al., 2021; Anjum et al., 2021).

1.7.5 Antibacterial property

Mutation, morphological and environmental change are the reason for the rise of multi-drug-resistant bacteria. Nanoparticles with antibacterial activity have the potential to decrease the evolution of these bacterial species by targeting numerous biomolecules and preventing the formation of resistant strains. Metal-based nanoparticles have antibacterial action mechanisms which include reactive oxygen species production, cation release and membrane interaction. Due to the lack of a sturdy layer of peptidoglycan found in the cell wall, damage caused by physical interactions between itself and the NPs is more severe in Gram-negative bacteria. Another reason for Gram-negative bacteria's vulnerability to NPs is because of the presence of a negative charge which has a greater affinity towards positive ions released by NPs which contributes to the absorption of ions which results in inner cell damage (Humann and Lenz, 2009). Iron oxide nanoparticles show enhanced antibacterial activity against gram negative bacteria. The main mechanism by which these particles showed antibacterial activity is because of oxidative stress generated by ROS. Damage to proteins and DNA in bacteria can be induced by ROS which includes superoxide radicals, hydroxyl radicals, hydrogen peroxide, and singlet oxygen (Wang et al., 2017).

1.7.6 Stability of iron oxide nanoparticles

There are several issues with IONPs, which include limited stability, particle aggregation, fast degradation, and magnetic property changes when they are exposed directly to systems-related biological properties. The zeta potential is the electrostatic potential at the boundary between the nanoparticle's compact and diffuse layers, according to (View of Synthesis and Characterization of Magnetic Iron Oxide Nanoparticles by Co-Precipitation Method at Different Conditions, no date b; Ostolska and Wiśniewska, 2014) It is used to assess the stability of NP suspensions. If all the particles in suspension have large negative or positive zeta potential then they will tend to repel each other and there will be no tendency for the particles to come together. Values in the –5 mV to + 5 mV range imply quick aggregation, according to Ostolska and Wiśniewska (2014).

2 Methodology

2.1 Preparation of nigella sativa seed extract

Preparation of a seed extraction by pre-treatment is an essential step in the extraction of thymoquinone by preparatory HPLC. A total of 3 different methods were used for the preparation of *N. sativa* seed extracts with various solvents. It was understood that using methanol, Hexane and aqueous extract as solvents for the process of seed extract had the highest yield of thymoquinone respectively, compared to other solvents like ethanol and benzene (Iqbal et al., 2018).

2.2 Pre-treatment of N. sativa using methanol as a solvent

Methanol is a polar solvent which is used extensively in the process of pre-treatment of *N. sativa* seeds. The seeds were dried and ground using an electric grinder by adding 10 mL of water to obtain a powder. 10 g of it was kept for soaking in 50 ml of methanol. The mixture was placed for stirring on a magnetic stirrer for 120 min. Filtration was performed using Whatman filter paper –1 with a pore size of 110 nm. Thymoquinone is a light-sensitive compound, on filtration store the yellow filtrate in a sealed and wrapped container at 4°C.

2.3 Pre-treatment of N. sativa using hexane as a solvent

A similar approach was used for the pre-treatment of the seeds using hexane as a solvent. The methanolic solvent was replaced with hexane and the resultant filtrate was stored in a sealed wrapped container at 4°C.

2.4 Preparation of aqueous extract from N. sativa seeds

Aqueous extraction refers to the soaking of seeds in distilled water and using this water for further analysis. 100 g of *N. sativa* seeds were dried and stored in a 500 mL glass beaker. 150 mL of distilled water was added to this and soaking was done for 24 h. The solution was then filtered using a Whatman filter paper –1 with a pore size of 110 nm. On filtration, the filtrate was sealed and wrapped in a container and store at 4°C

2.5 Preparatory high-pressure liquid chromatography for extraction of thymoquinone

Reversed-phase preparative HPLC was carried out using Shimadzu SIL10 AP and an LC- 20AP pump system with a UV detector at "The Bangalore Bio-Innovation Centre". The separation was performed on a Sunfire C18 column. UV detection was carried out at 254 nm with an injection volume of 58.07 ml. The mobile phase was consisting of methanol as solvent A and water containing 0.1% TFA as solvent B. The gradient program set in the software is shown in Table 1.

Table 1 Shows the concentration gradient and the time period for each

Concentration	*Time period*
5%	10 min
50%	After 10 min
50%	Retained for 10 min
100%	After 5 min
100%	Retained for 5 min
5%	5 min

Source: Ghanavi et al. (2020)

2.6 Synthesis of iron oxide nanoparticles

5.6 g of Ferric chloride hexahydrate and 6.7 g of ferrous sulphate were dissolved in 50 ml of 0.5M HCl. 90 ml of 1.5M Sodium Hydroxide solution was added dropwise to the solution which was under vigorous mixing on a hot plate stirrer set at 80°C and 100 rpm. The pH of the solution was observed to be highly basic (pH 12), on obtaining a viscous and jet-black colouration, transfer the solution to 50 ml centrifuge tubes. Approximately 83 mL of Sodium Hydroxide was needed to obtain the viscous jet-black coloured precipitate. Centrifuge the solution at 2000 rpm for 2 min. Followed by the washing step where we discard the supernatant and add 10 ml of distilled water and dislodge the pallet. Perform the washing step 5–6 times until the pH of the solution is neutral (pH 6.5). Finally, discard the supernatant and transfer the pellet to a Petri plate and place it in a hot air oven set to 60°C for strictly 8 h to avoid crystallisation. Scrape out the powdered particles using a sterilised spatula and store them in 1.5 ml tubes away from sunlight.

2.6.1 Synthesis of iron oxide

Nanoparticles using *Nigella sativa* (Methanolic extract) 5.6 g of Ferric chloride hexahydrate and 6.7 g of ferrous sulphate were dissolved in 50 ml of 0.5M HCl. 10 mL of the prepared methanolic extract was added. 90 ml of 1.5M Sodium Hydroxide was added dropwise to the solution which is under vigorous mixing on a hot plate stirrer set at 80°C and 100 rpm. The pH of the solution was observed to be highly basic (pH 12), on obtaining a viscous and jet-black colouration, transfer the solution to 50 ml centrifuge tubes. Around 83 mL of Sodium Hydroxide was needed to obtain the viscous jet-black

coloured precipitate. Centrifuge the solution at 2000 rpm for 2 min. Followed by the washing step where we discard the supernatant and add 10 ml of distilled water. Perform the washing step 5–6 times until the pH of the solution is neutral (pH 6.5). Make sure the sides of the centrifuge tubes are sealed with Aluminium foil to prevent light exposure as Thymoquinone is light sensitive. Finally, discard the supernatant and transfer the pellet to a Petri plate and place it in a hot air oven set at 60°C for strictly 8 h to avoid crystallisation. Scrape out the particles using a sterilised spatula and store it in a 1.5 ml sealed tube away from sunlight.

2.6.2 Synthesis of Iron Oxide Nanoparticles using Nigella sativa (Hexane extract)

A similar procedure as mentioned above was administered and 10 mL of the prepared Hexane extract was added following which the nanoparticles were dried and scraped out.

2.6.3 Synthesis of iron oxide nanoparticles using Nigella sativa seeds (Aqueous extract)

A similar procedure as mentioned above was administered and 10 mL of the prepared Aqueous extract was added following which the nanoparticles were dried and scraped out and stored in an airtight tube away from sunlight.

2.6.4 Synthesis of iron oxide nanoparticles using DMSO dissolved in thymoquinone

A similar procedure of synthesis was followed after which 5 mL of thymoquinone in DMSO (1 : 1 ratio) was added to the solution and stirred at 120 rpm (No heat to be provided) following which the nanoparticles were dried and scraped out and stored in an airtight tube away from sunlight.

2.7 Characterisation study

Characterisation was performed on the size of nanoparticles obtained, zeta potential and FTIR analysis on the synthesised nanoparticles with the different extracts and the pure thymoquinone obtained by preparatory HPLC.

2.7.1 Size analysis by dynamic light scattering (DLS)

The prepared particles were analysed at “Nargund College of Pharmacy, Bangalore” using the Horiba SZ-100 nanoparticle size analyses. The literature review suggested that the iron oxide nanoparticles are to be in the size range below 100 nm. The SZ-100 works on the principle of DLS. DLS is the measurement of fluctuations in scattering light intensity with respect to time. These fluctuations arise due to the presence of Brownian movement of the nanoparticles in the suspension. The statistical behaviour of these fluctuations in scattering intensity can be related to the diffusion of particles. Larger particles diffuse slower than smaller ones and thus we can relate them to the particle size.

2.7.2 Working procedure for the apparatus

Dilute 0.005 g of the sample in 10 ml of distilled water and load the solution into the cuvette. Place the cuvette in the loading spot on the apparatus. Run the software to obtain a graph on the average value of the size of particles present.

2.7.3 Stability analysis by zeta potential measurement

Zeta Potential was used to analyses the stability of the nanoparticles. The prepared particles were analysed at "The Nargund College of Pharmacy" using the Horiba SZ-100 nanoparticle size analyser. The measurement range varies from –200 mV to +200 mV. Zeta potential cells which contain electrodes were used. Light scattering is used to determine the particle motion caused by the applied electric field. The laser light illuminates the particles, and as a result, the particles scatter light. Due to the Doppler shift, the frequency of the scattered light depends on the particle velocity. To accurately extract the frequency shift in the scattered light, a second beam of light – referred to as the reference beam – is mixed with the dispersed beam. A small amount of suspension is added to the measuring cell before it is inserted into the instrument to take the measurement. In order to achieve the best signal-to-noise ratio, the instrument software then automatically selects the proper electric field strength, modifies the reference beam intensity, gathers, and analyses the data, and displays the findings to the user. The impact of H + or other ions on zeta potential is frequently significant.

2.7.4 Working procedure for the apparatus

Dilute 0.005 g of the sample in 10 ml of distilled water and load the solution into the cuvette. Place the cuvette in the loading spot on the apparatus. Run the software to obtain a graph and zeta potential of particles.

2.7.5 Fourier-transform infrared spectroscopy for analysis of samples

Fourier-transform infrared spectroscopy is an analysis method to identify the presence of certain functional groups in a given sample. Analysis for the obtained sample from preparatory HPLC was tested for its functional groups using FTIR. Shimadzu FTIR-8400 s apparatus was used at "Nargund college of Pharmacy, Bangalore"

2.7.6 Sample preparation (Liquid)

Potassium bromide (KBr) is a lead compound used in the process of FTIR. The ratio for the sample to the KBr used is 1 : 100. Take two stainless steel discs from the desiccator and place a piece of cardboard between the plates followed by the addition of thymoquinone ground with the KBr. Place this sandwich into a hydraulic press with a pressure of 100psi to obtain a neat clean pellet. Transfer this pallet into the sample loading spot of the machine and run the software to obtain a spectrum.

2.7.7 Sample preparation (Solid)

The ratio for the sample to the Potassium Bromide (KBr) used is 1 : 100. Take two stainless steel discs from the desiccator and place a piece of cardboard between the plates

followed by the addition of various prepared iron oxide nanoparticles samples ground with the KBr. Place this sandwich into a hydraulic press with a pressure of 100psi to obtain a neat clean pellet. Transfer this pallet into the sample loading spot of the machine and run the software to obtain a spectrum.

3 Results and discussion

Thymoquinone in *Nigella sativa* seeds and Iron oxide nanoparticles both show antibacterial activity against gram-negative species of bacteria. The aim of this research was the combine these two compounds to bring about a broader array of antibacterial activity against these deadly disease- causing bacteria.

3.1 Preparatory high-pressure liquid chromatography for extraction ofthymoquinone

Since literature reviews suggest methanol to be the best solvent for the process of extraction preparatory HPLC was done only for this extract. On comparing the standard thymoquinone graph obtained from the literature review, the extraction of thymoquinone is at a retention time of approximately 30 min from the start of the procedure.

Thymoquinone analysis is to be done at a wavelength of 254 nm. A clear peak of thymoquinone was obtained at a retention time of 29 min and the resultant extract was collected in a sealed wrapped contained and stored immediately at 4°C. The resultant graph has been depicted in Figure 1.

Figure 1 Preparatory HPLC graph obtained for methanolic extract (see online version for colours)

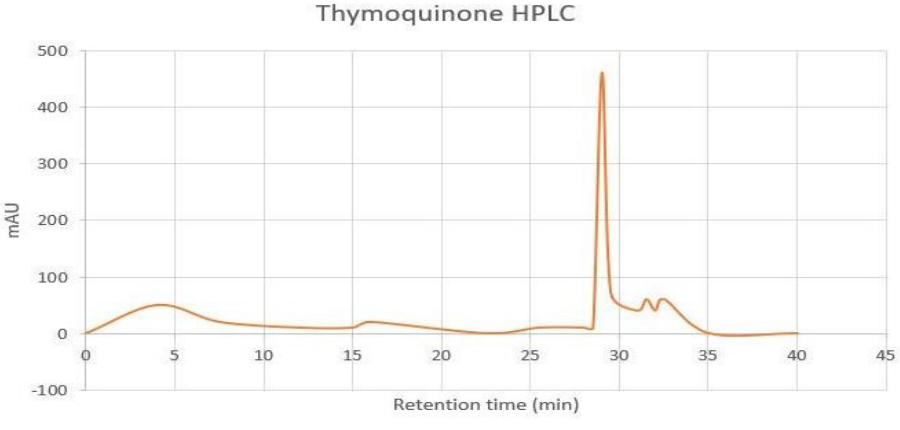

A standard graph for thymoquinone was used to compare the obtained peaks (Ghanavi et al., 2020). On comparing it was observed that the retention time for thymoquinone is at 29 min, thus we can conclude the extraction of thymoquinone from HPLC, a detailed FTIR analysis has been performed to confirm the presence of the different functional groupsof thymoquinone from this extract.

FTIR Analysis Fourier Transform infrared spectroscopy was performed to check for the presence of Thymoquinone and iron oxide nanoparticles functional groups. Further the synthesised nanoparticles with thymoquinone were also subjected to FTIR to compare and conclude on the best solvent for thepreparation of the concoction.

Thymoquinone The obtained graph from FTIR analysis Figure 2 were compared to the standard peaks from (Rani et al., 2018), and a comparative tabulated result was obtained in Table 2.

Figure 2 Graph obtained for the FTIR of thymoquinone extracted bypreparatory HPLC (see online version for colours)

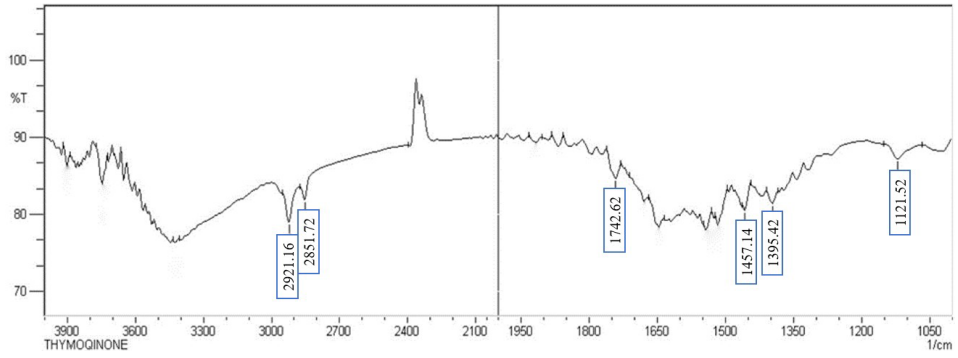

Table 2 Comparison for the values obtained and the standard values ofthymoquinone

Intensity fromliterature review (Rani et al., 2018)	Obtainedintensity	Depiction
3000 cm^{-1} to 2800 cm^{-1}	3000 cm^{-1} to 2800 cm^{-1}	Stretching vibrations of the isopropyl and CH_3 groups
2924.81 cm^{-1}	2921.16 cm^{-1}	C–H stretching of tertiary carbon in the isopropyl group
2856.13 cm^{-1}	2851.72 cm^{-1}	Presence of the three methyl groups
1711.23 cm^{-1}	1742.82 cm^{-1}	C = O stretching
1459.31 cm^{-1}	1457.14 cm^{-1}	CH_3 antisymmetric bending
1383.68 $cm^{-1}$and 1354.22 cm^{-1}	1395.42 cm^{-1}	Symmetric bending of tertiary carbon in the isopropyl group
1100–900 cm^{-1}	1121.52 cm^{-1}	CH_3 rocking

On comparing the peaks and their significant, it is observed that the obtained peaks are in very close agreement with the literature values(Rani et al., 2018).

3.2 Iron oxide nanoparticles

FTIR was performed on the pure iron oxide nanoparticles synthesized from 2.6 and the resulting graph with a comparative table have been shown (Figure 3, Table 3).

Figure 3 FTIR graph for pure iron oxide nanoparticles (see online version for colours)

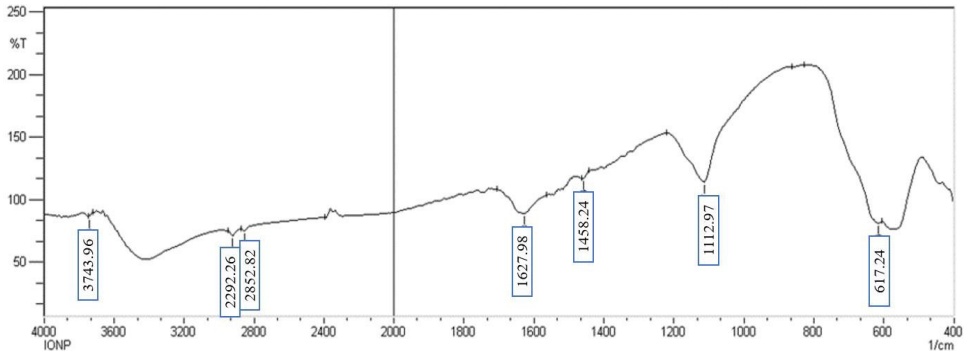

Table 3 Comparing values from literature and obtained

FT-IR (*Literature*) (*Rani et al., 2018*)	*FT-IR Obtained*	*Functional Group*
602 cm^{-1}	617 cm^{-1}	Fe-O
3398 cm^{-1}	3410 cm^{-1}	O-H
2359 cm^{-1}	2360 cm^{-1}	C-O
1621 cm^{-1}	1627.98 cm^{-1}	N-H
1033 cm^{-1}	1112.97 cm^{-1}	C-H

3.3 Methanolic iron oxide nanoparticles

Four different peaks were obtained 576.74 cm^{-1} for Fe-O, 1107.18 cm^{-1} for CH_3, 1460 cm^{-1} for CH_3 antisymmetric bending and 2920.33 cm^{-1} corresponding to C-H stretching of tertiary carbon in isopropyl group which are in argument with the literature reviewed (Rani et al., 2018) (Figure 4).

Figure 4 FTIR graph for methanolic iron oxide nanoparticles (see online version for colours)

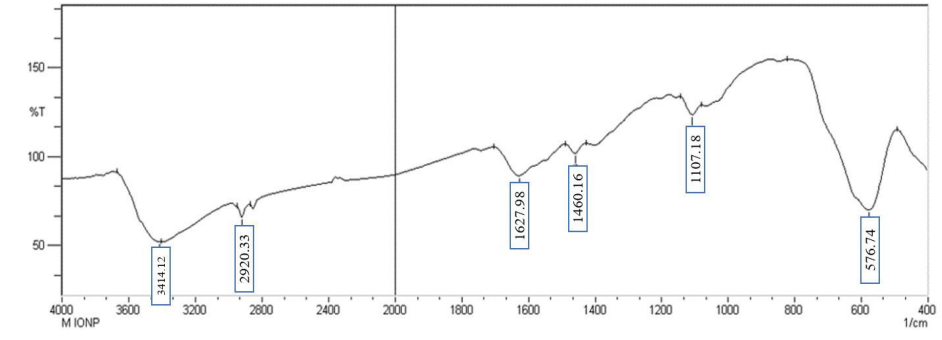

3.4 Hexane iron oxide nanoparticles

FTIR was performed on the iron oxide nanoparticles synthesised using hexane as a solvent from 2.6.2 and the resulting graph with a comparative table have been shown (Figure 5, Table 4).

Figure 5 FTIR graph for hexane iron oxide nanoparticles (see online version for colours)

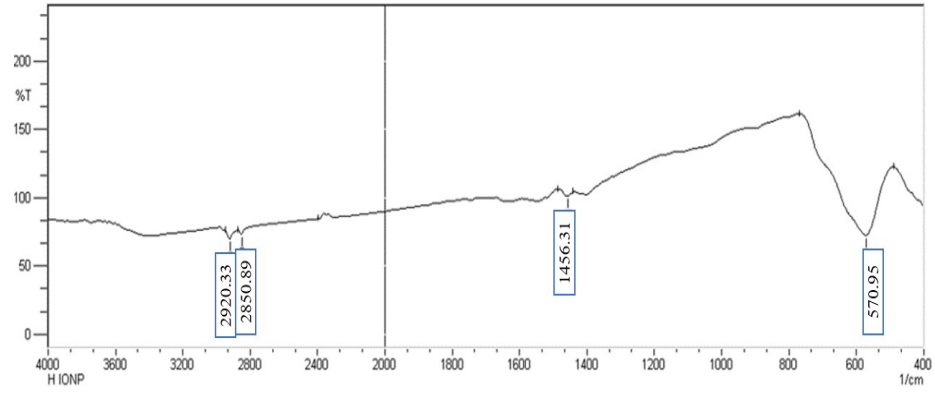

Table 4 Comparing values from literature and obtained for hexane IONP

FT-IR (Literature) (Rani et al., 2018)	*FT-IR obtained*	*Functional group*
576 cm^{-1}	570.95 cm^{-1}	Fe-O
1459.31 cm^{-1}	1456.31 cm^{-1}	CH_3 antisymmetric bending
2856.13 cm^{-1}	2850.89 cm^{-1}	Three CH_3 Groups symmetric stretching
2926.23 cm^{-1}	2920.33 cm^{-1}	C-H stretching of tertiary carbon inisopropyl group

3.5 Aqueous iron oxide nanoparticles

FTIR was performed on the aqueous iron oxide nanoparticles from 2.6.3 and the resulting graph with a comparative table has been shown (Figure 6, Table 5).

Figure 6 FTIR for aqueous iron oxide nanoparticles (see online version for colours)

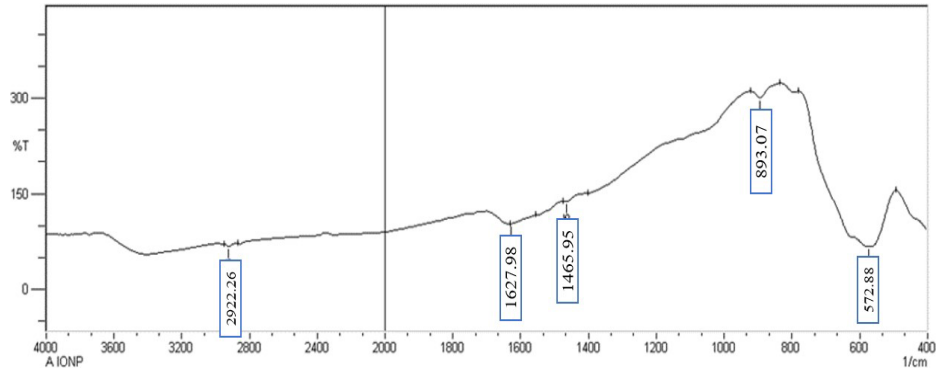

Table 5 Comparing values from literature and obtained for aqueous IONP

FT-IR (*Literature*) (*Rani et al., 2018*)	*FT-IR Obtained*	*Functional group*
576 cm^{-1}	572.88 cm^{-1}	Fe-O
1459.31 cm^{-1}	1465.95 cm^{-1}	CH_3 antisymmetric bending
2926.23 cm^{-1}	2922.6 cm^{-1}	C-H stretching of tertiary carbon inisopropyl group

3.6 DMSO- thymoquinone iron oxide nanoparticles

FTIR was performed on the DMSO dissolved iron oxide nanoparticles from 2.6.4 and the resulting graph with a comparative table have been shown (Figure 7, Table 6).

On comparing the FTIR results it is observed that the different functional groups present in DMSO dissolved in Thymoquinone IONP (Table 6) were in close relations with the native Thymoquinone and Iron oxide nanoparticles from (Tables 2 and 3). Further to confirm the stability and aggregation of the nanoparticles Zeta potential analysis was performed.

Figure 7 FTIR for DMSO-thymoquinone iron oxide nanoparticles (see online version for colours)

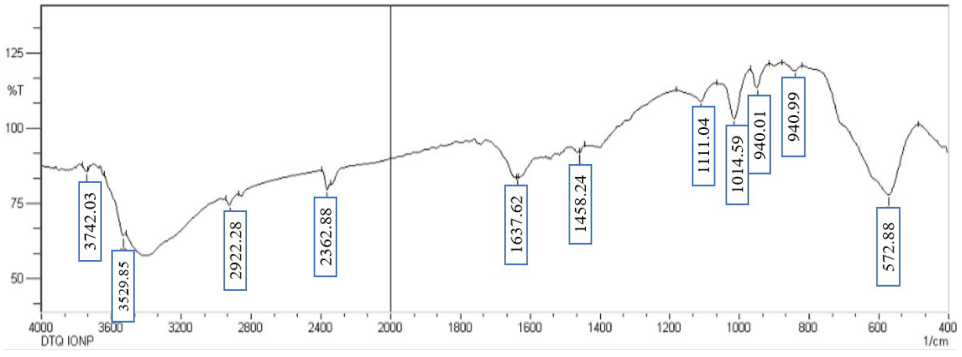

Table 6 Comparing values from literature and obtained for DMSO-thymoquinone IONP

FT-IR (*Literature*) *(Rani et al., 2018)*	*FT-IR Obtained*	*Functional Group*
576 cm^{-1}	572.88 cm^{-1}	Fe-O
1100–900 cm^{-1}	1111.04 cm^{-1}	CH_3
1459.31 cm^{-1}	1458.24 cm^{-1}	CH_3 antisymmetric bending
2924.81 cm^{-1}	2922.26 cm^{-1}	C-H stretching of tertiary carbon inisopropyl group
3009 cm^{-1}	3529.85 cm^{-1}	CH stretching of the vinyl group

3.7 Dynamic light scattering

Five Samples were considered for Analysis to check for their size: Iron Oxide Nanoparticles (IONP), Methanolic Extract Iron Oxide Nanoparticles (MIONP), Hexane Extract Iron Oxide Nanoparticles (HIONP), Aqueous Extract Iron Oxide Nanoparticles (AIONP), DMSO- Thymoquinone Iron Oxide Nanoparticles (DMSO- TIONP). The Obtained results are tabulated (Table 7).

Table 7 Size analysis

Samples	*Size obtained*	*Polydispersityindex*
IONP	65.3 nm	3.056
MIONP	63.6 nm	3.019
HIONP	63.1 nm	2.816
AIONP	66.8 nm	3.053
DMSO-TIONP	71.8 nm	2.992

3.8 Zeta potential

Five Samples were considered for Analysis: Iron Oxide Nanoparticles (IONP), Methanolic Extract Iron Oxide Nanoparticles (MIONP), Hexane Extract Iron Oxide Nanoparticles (HIONP), Aqueous Extract Iron Oxide Nanoparticles (AIONP), The obtained results are tabulated in Table 8.

Table 8 Zeta potential analysis

Samples	*Zeta potential*
IONP	12.5 mV
MIONP	5.5 mV
HIONP	–11.8 mV
AIONP	–8.0 mV
DMSO-TIONP	15.1 mV

Three most efficient processes were adopted for the characterisation of the synthesised nanoparticles. FTIR to check for the functional groups present, DLS to check for the size and Zeta potential to confirm the overall stability of the nanoparticles synthesised. DLS gave an overall size below 100 nm and the corresponding polydispersity Index for the synthesised nanoparticles.

4 Conclusion

Nigella sativa is a plant which has gained immense attention in the field of traditional medicine and has been used in India as a part of Ayurveda to treat the sick. Thymoquinone is one of the main compounds present in the seeds of this plant which is responsible for bringing about phytochemical activity in humans. Iron Oxide

nanoparticles on the other hand have been used extensively in the field of medical science for their benefits of being anticancer, antibacterial, anti-fungal and anti-inflammatory. Synthesising these two natural compounds by novel methods and comparing the yield, purity and size of the compounds obtained has been the primary aim of this research. Gram-negative bacteria have been the lead microorganisms which cause diseases in humans, resistance against these microorganisms has been a prime aim of the commercially available antibiotics. They have been successful but come at a cost of several side effects. Extraction of Thymoquinone was done using 3 different solvents namely Methanol, Hexane, and an aqueous extract to compare the yield from these 3 compounds. It was understood that methanol gave the highest yield of thymoquinone due to which preparatory HPLC was performed only for this sample. Preparatory HPLC was carried out successfully and Thymoquinone was obtained at a retention time of 30 min. This was further confirmed by performing FTIR for the extract and obtaining promising results for the different functional groups when compared to the available literature. On combining all these samples with iron oxide nanoparticles FTIR was performed which confirmed the fact that Thymoquinone dissolved in DMSO- IONP gave the best result followed by methanol and hexane and the least efficient extraction was by the aqueous extract. Size analysis was performed and all the samples were within the 60 to 70nm range. Zeta Potential analysis was done to check for the stability of the samples obtained the most stable being DMSO-Thymoquinone Iron oxide nanoparticle with 15.1mV. As mentioned earlier than pH affects zeta potential values. Author Since IONP is neutral the zeta potential value is higher 12.5 mV which indicates stability. In MIONP, *Nigella sativa* seed extract is acidic (negatively charged) and the pH of methanol depends on the concentration of methanol (pH increases as the concentration increases) and the drying of the nanoparticles in a hot air oven could have decreased pH (increase in temperature reduction in pH), would have led to reduction its zeta potential to 5.5mV (pH in Methanol, no date). In HIONP Hexane is a non-polar compound and it has a neutral pH so the sample is completely acidic due to the negatively charged *Nigella sativa* and also the drying could have also impacted the pH, therefore, the value is – 11.8 mV. Thymoquinone though neutral but because of its instability and light sensitivity and traces of impurities during HPLC extraction could have caused fluctuations in pH and reduced the zeta potential drastically leading to instability TQ IONP. The reason for adding DMSO is that it dissolves thymoquinone and it is highly alkaline which could counteract the negatively charged *Nigella sativa* and increase stability. The aim of the current research was to prepare stable aggregates of Thymoquinone iron oxide nanoparticles, this research can be further extended to test for their antibacterial activity on various gram-negative species of bacteria. In conclusion all the three methods used for characterisation can help in proving the size, functional group, and the stability of the synthesised nanoparticles, all of which are essential to test for their antibacterial activity. Which is the future prospectus of this study.

Acknowledgements

Sheshadri S. Temkar, M. Tarun, Seema Tharannum have contributed equally to this work.

References

'Antibiotic resistance–the problem intensifies' (2005) *Advanced Drug Delivery Reviews*, Vol. 57, No. 10, pp.1446–1450.

Ahmad, A., Husain, A., Mujeeb, M., Khan, S.A., Najim, A.K., Siddique, N.A., Damanhouri, Z.A. and Anwar, F. (2013) 'A review on therapeutic potential of *Nigella Sativa*: a miracle herb', *Asian Pacific Journal of Tropical Biomedicine*, Vol.3, No. 5, pp.337–352.

Ali, A., Zafar, H., Zia, M., ul Haq, I., Phull, A.R., Ali, J.S., Hussain, A. *et al.* (2016) 'Synthesis, characterization, applications, and challenges of iron oxide nanoparticles', *Nanotechnology, Science and Applications*, Vol. 9, p.49.

Ali, B.H. and Blunden, G. (2003) 'Pharmacological and toxicological properties of *Nigella Sativa*', *Phytotherapy Research: PTR*, Vol. 17, No. 4, pp.299–305.

Anjum, S., Hashim, M., Malik, S.A., Khan, M., Lorenzo, J.M., Abbasi, B.H. and Hano, C. (2021) 'Recent advances in zinc oxide nanoparticles (ZnO NPs) for cancer diagnosis, target drug delivery, and treatment', *Cancers*, Vol. 13, No. 18, Available at. https://doi.org/10.3390/cancers13184570

Balyan, P., Shinde, S. and Ali, A. (2021) 'Potential activities of nanoparticles synthesized from *Nigella Sativa*, L and its phytoconstituents:an overview', *Journal of Phytonanotechnology and Pharmaceutical Sciences*, Available at. https://doi.org/10.21276/jpps.2021.1.2.1

Bita, A., Rosu, A.F., Calina, D., Rosu, L., Zlatian, O., Dindere, C. and Simionescu, A. (2012) 'An alternative treatment for candida infections with *Nigella Sativa* extracts', *European Journal of Hospital Pharmacy. Science and Practice*, Vol. 19, No. 2, pp.162–162.

Department of Health and Human Services (no date) *Antibiotic Resistant Bacteria*, Available at. http://www.betterhealth.vic.gov.au/health/conditionsandtreatments/antibiotic-resistant-bacteria (Accessed 29 May, 2023).

Dinali, R., Ebrahiminezhad, A., Manley-Harris, M., Ghasemi, Y. and Berenjian, A. (2017) 'Iron oxide nanoparticles in modern microbiology and biotechnology', *Critical Reviews in Microbiology*, Vol. 43, No. 4, pp.493–507.

Forouzanfar, F., Bazzaz, B.S.F. and Hosseinzadeh, H. (2014) 'Black cumin (*Nigella Sativa*) and its constituent (thymoquinone): a review on antimicrobial effects', *Iranian Journal of Basic Medical Sciences*, Vol. 17, No. 12,p.929.

Ghanavi, Z., Velayati, A.A., Farnia, P., Naji, A.M. and Kalatehjari, S. (2020) 'Extraction and purification of anticancer thymoquinone from seeds of *Nigella Sativa* by preparative high-performance liquid chromatography', *Journal of Medicinal Plants and By-Product*, Vol. 9, Special, pp.73–79.

Howden, B.P., Davies, J.K., Johnson, P.D.R., Stinear, T.P. and Lindsay Grayson, M. (2010) 'Reduced vancomycin susceptibility in staphylococcus aureus, including vancomycin-intermediate and heterogeneous vancomycin-intermediate strains: resistance mechanisms, laboratory detection, and clinical implications', *Clinical Microbiology Reviews*, Vol. 23, No. 1, pp.99–139.

Humann, J. and Lenz, L.L. (2009) 'Bacterial peptidoglycan degrading enzymes and their impact on host muropeptide detection', *Journal of Innate Immunity*, Vol. 1, No. 2, p.1, Available at. https://doi.org/10.1159/000181181

Iqbal, M.S., Ahmad, A. and Pandey, B. (2018) 'Solvent based optimization for extraction and stability of thymoquinone from *Nigella Sativa* linn. and its quantification using RP-HPLC', *Physiology and Molecular Biology of Plants: An International Journal of Functional Plant Biology*, Vol. 24, No. 6, pp.1209–1219.

Łopusiewicz, Ł., Śmietana, N., Paradowska, D. and Drozłowska, E. (2022) 'Black cumin (*Nigella Sativa*, L) seed presscake as a novel material for the development of new non-dairy beverage fermented with kefir grains', *Microorganisms*, p.300, Available at: https://doi.org/10.3390/microorganisms10020300

[No title] (no date) Available at. https://citeseerx.ist.psu.edu/document?repid=rep.1& type=pdf & doi=3127f4 f6ffa0824e366334475f3b784be9a14fd3 (Accessed 29 May, 2023).

Oliveira, J. and Reygaert, W.C. (2019) *Gram Negative Bacteria*, Available at. https://europepmc.org/article/NBK/nbk538213?client=bot(Accessed 12 December, 2022).

Ostolska, I. and Wiśniewska, M. (2014) 'Application of the zeta potential measurements to explanation of colloidal Cr2O3 stability mechanism in the presence of the ionic polyamino acids', *Colloid and Polymer Science*, Vol. 292, No. 10, pp.2453–2464'.

'Nanoparticles: Properties, applications and toxicities' (2019) *Arabian Journal of Chemistry*, Vol. 12, No. 7, pp.908–931.

pH in Methanol (no date) Available at. https://www.yokogawa.com/in/library/resources/application-notes/ph-in-methanol/ (Accessed 28 February, 2023).

Rani, R., Dahiya, S., Dhingra, D., Dilbaghi, N., Kim, K-H. and Kumar, S. (2018) 'Improvement of antihyperglycemic activity of nano-thymoquinone in rat model of type-2 diabetes', *Chemico-BiologicalInteractions*, Vol. 295, pp.119–132.

Shokri, H. (2016) 'A review on the inhibitory potential of *Nigella Sativa* against pathogenic and toxigenic fungi', *Avicenna Journal of Phytomedicine*, Vol. 6, No. 1, p.21.

Sun, Y., Ma, X., Jing, X. and Hu, H. (2021) 'PAMAM-functionalized cellulose nanocrystals with needle-like morphology for effective cancer treatment', *Nanomaterials*, Vol. 11, No. 7, p.1640.

'Thymoquinone and its therapeutic potentials' (2015) *Pharmacological Research: The Official Journal of the Italian Pharmacological Society*, Vols. 95–96, pp.138–158.

'Thymoquinone: Potential cure for inflammatory disorders and cancer' (2012) *Biochemical Pharmacology*, Vol. 83, No. 4, pp.443–451.

Tran, N., Mir, A., Mallik, D., Sinha, A., Nayar, S. and Webster, T.J. (2010) 'Bactericidal effect of iron oxide nanoparticles on staphylococcus aureus', *International Journal of Nanomedicine*, Vol. 5, p.277.

Tubesha, Z., Bakar, Z.A. and Ismail, M. (2013) 'Characterization and stability evaluation of thymoquinone nanoemulsions prepared by high-pressure homogenization', *Journal of Nanomaterials*, Vol. 2013, pp.1–6, Available at: https://doi.org/10.1155/2013/453290

View of Synthesis, and Characterization of Magnetic Iron Oxide Nanoparticles by Co-Precipitation Method at Different Conditions (no date a) Available at. https://www.joe.uobaghdad.edu.iq/index.php/main/article/view/j.eng.2018.10.05/536 (Accessed 12 December, 2022).

View of Synthesis, and Characterization of Magnetic Iron Oxide Nanoparticles by Co-Precipitation Method at Different Conditions (no date b). Available at. https://www.joe.uobaghdad.edu.iq/index.php/main/article/view/j.eng.2018.10.05/536 (Accessed 12 December, 2022).

Wang, L., Hu, C., Shao, L. (2017) 'The antimicrobial activity of nanoparticles: present situation, prospects for the future', *InternationalJournal of Nanomedicine*, Vol. 12, p.1227.

Waterer, G.W. and Wunderink, R.G. (2001) 'Increasing threat of gram-negative bacteria', *Critical Care Medicine*, Vol. 29, No. 4, p.N75.

Website (no date) Available at https://www.jstor.org/stable/24103844

Yoshikawa, T.T. (2002) 'Antimicrobial resistance and aging: beginning ofthe end of the antibiotic era?', *Journal of the American Geriatrics Society*, Vol.50, 7 Suppl, pp.S226–S229.

Zgurskaya, H.I., Löpez, C.A. and Gnanakaran, S. (2015) 'Permeability barrier of gram-negative cell envelopes and approaches to bypass it', *ACS Infectious Diseases*, Vol. 1, No. 11, pp.512–522.